

Engineering Notes

ENGINEERING NOTES are short manuscripts describing new developments or important results of a preliminary nature. These Notes should not exceed 2500 words (where a figure or table counts as 200 words). Following informal review by the Editors, they may be published within a few months of the date of receipt. Style requirements are the same as for regular contributions (see inside back cover).

Automated Process for Optimal Structural Notch-Filter Design

G. K. Singh*

National Aerospace Laboratories,
Council of Scientific and Industrial Research,
Bangalore 560 017, India

Girish Deodhare[†] and Vijay V. Patel[‡]
Aeronautical Development Agency,
Bangalore 560 017, India

and

Shyam Chetty[§]

National Aerospace Laboratories,
Council of Scientific and Industrial Research,
Bangalore 560 017, India

DOI: 10.2514/1.36767

Nomenclature

C, C_{ij}	=	controller transfer function, i, j element of C
de, da, dr	=	elevator, aileron, and rudder surface deflections
F_k	=	k th second-order filter section
fs	=	sampling frequency
m_x	=	variable magnitude for sensor x
Nz, Ny	=	normal, lateral acceleration
P, P_{ij}	=	plant transfer function, i, j element of P
p, q, r	=	roll, pitch, and yaw rates
w, w_c	=	frequency variable, critical frequency
w_x	=	weight factor for sensor x
X_{env}	=	envelope for sensor X
X_F, X_{NF}	=	filter (notch filter) for sensor X
ζ_n, ζ_d	=	damping of the numerator/denominator
ω_n, ω_d	=	natural frequency of the numerator/denominator

I. Introduction

THE term “structural coupling” refers to the interactions between the flight control system (FCS), the structural dynamics, and the airframe aerodynamics. The FCS motion sensors will sense not only the rigid-body motion of the aircraft but also the flexible modes of the

structure on which they are mounted. These high-frequency signals, if not properly attenuated, could be amplified in a closed loop and could lead to instabilities at the structural frequencies. The desire for increased agility and lightweight structures has reduced the gap between the rigid-body and structural frequencies; hence, structural-coupling effects have become more pronounced. Additional notch filters are introduced in the sensor feedback paths to attenuate the effects of structural coupling. Special ground tests called structural coupling tests (SCT) are carried out on the fully equipped aircraft to quantify the structural modes picked up by the inertial sensors, and these experimental data are used for the design of the notch filters.

This paper describes the design of the structural notch filters for a generic fighter aircraft with an emphasis on minimizing phase lag at rigid-body gain crossover frequency, which is typically around 1 Hz, while meeting the structural stability gain margin requirement of 8 dB (gain stabilization) as stated in MIL-F-9490D [1]. These notch filters can introduce significant phase lag at the rigid-body gain crossover frequency, which affects the stability of the rigid-body dynamics, and hence the additional phase lags are minimized. It is assumed that the structural modes are sufficiently separated from rigid-body modes, thereby making gain stabilization feasible.

In [2], a suboptimal strategy for the design of notch filters for the coupled lateral/directional axes of an aircraft was presented. The conventional design methods are mostly based on trial and error or a loop-by-loop design and often lead to a very conservative design. Mehra et al. [3] and Le Garrec and Kubica [4] discuss methods of in-flight structural mode identification for adaptive notching of structural modes. However, traditionally one relies on the results obtained from structural coupling tests to obtain the structural modal parameters, followed by an offline design of notch filters. Mehra et al. [3] and Halsey and Goodall [5] present an alternative approach using Kalman filtering to estimate the rigid-body component from the sensor measurements. However, this method relies on the accurate knowledge of the rigid-body modes. Hoffmann [6] used genetic-evolutionary algorithms for designing notch filters for one sensor path with an assumed number of filter sections.

In this paper, a novel approach to the design of the structural notch filters in the presence of coupling between all three axes is proposed. The notch-filter design problem is formulated as a two-step optimization process. The first step finds the optimal attenuation required (at each discrete frequency point) in each of the sensor paths while meeting the stability margin requirement for gain stabilization. These are collated over the frequency range to generate “optimal” attenuation envelopes. The theoretical minimum phase lag for these attenuation envelopes can be easily computed using the famous Bode’s gain-phase relationship. This significantly accelerates the entire design process by facilitating a multi-objective tradeoff in systematic design exercise. The second step involves the design of individual notch filters for the various sensor paths so as to meet these optimal attenuation envelopes while minimizing the phase lag at 1 Hz (rigid-body gain crossover frequency) contributed by these filters. The effect of the number of filter sections in a sensor path and the resulting phase lag has also been studied. This work is an extension of our results presented in [7].

II. Structural Response and Bounds on Gain Margins

The controller inputs are the five plant outputs, namely, the pitch rate (q), normal acceleration (Nz), the roll rate (p), the yaw rate (r),

Received 22 January 2008; revision received 25 February 2008; accepted for publication 3 March 2008. Copyright © 2008 by the American Institute of Aeronautics and Astronautics, Inc. All rights reserved. Copies of this paper may be made for personal or internal use, on condition that the copier pay the \$10.00 per-copy fee to the Copyright Clearance Center, Inc., 222 Rosewood Drive, Danvers, MA 01923; include the code 0731-5090/08 \$10.00 in correspondence with the CCC.

*Scientist, Flight Mechanics and Control Division; gksingh@css.nal.res.in.

[†]Scientist, Integrated Flight Control System Directorate, Post Box 1718; gsdeodhare@gmail.com.

[‡]Scientist, Integrated Flight Control System Directorate, Post Box 1718; vvp2069@yahoo.com.

[§]Scientist, Flight Mechanics and Control Division; shyam@css.nal.res.in.

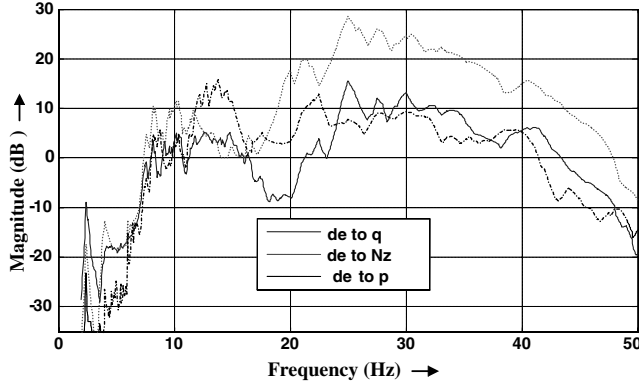


Fig. 1 Typical structural frequency response plots from elevator inputs.

and the lateral acceleration (N_y). The controller outputs are the elevator, aileron, and rudder deflection commands (de , da , and dr).

The servo-elastic structural response data measured in SCT consists of 15 transfer functions from the three control inputs to the five sensor outputs. Typical worst-case structural response plots across all the tested configurations for the elevator excitations are shown in Fig. 1. It can be seen that the magnitude of the cross transfer functions (i.e., de to p) is of the same order as the direct transfer functions (i.e., de to q and de to N_z). A combination of analog and digital notch-filter sections is provided in the acceleration and rate sensor paths. An analog notch-filter section is required to cater for the attenuation requirements in the band 30–50 Hz, in which the performance of the digital filters degrades significantly around half the sampling frequency (40 Hz).

The structural model of the aircraft (P), the notch filters (placed in sensor feedback paths), and the controller (C) are shown in Fig. 2. The margins are calculated (as per MIL-F-9490D) by breaking the loop at one sensor/actuator consolidation point at a time with the remaining loops closed. The figure shows a schematic for obtaining the pitch rate sensor margin by opening the loop at the pitch rate (q) sensor with all the other loops closed. Gain margins for the other loops can be similarly evaluated by opening one loop at a time with the other loops closed.

As discussed earlier, the notch-filter design is intended for gain stabilization, and hence a tight bound on the true gain margin using only the magnitude information is required. The bounds on the structural stability margins in the actuator paths are computed using the method proposed in [7] for the case of three inputs and three outputs (the 3×3 case). The sensor stability margins require results for the 5×5 case. Let the loop transfer function be given by L , which has the following form:

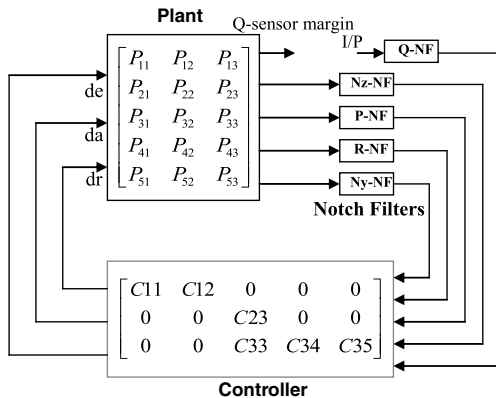


Fig. 2 Plant, controller, and notch filters with Q -sensor loop open.

$$\begin{aligned} q &\rightarrow [L_{11} \ L_{12} \ L_{13} \ L_{14} \ L_{15}] \rightarrow q' \\ N_z &\rightarrow [L_{21} \ L_{22} \ L_{23} \ L_{24} \ L_{25}] \rightarrow N'_z \\ p &\rightarrow [L_{31} \ L_{32} \ L_{33} \ L_{34} \ L_{35}] \rightarrow p' \\ r &\rightarrow [L_{41} \ L_{42} \ L_{43} \ L_{44} \ L_{45}] \rightarrow r' \\ N_y &\rightarrow [L_{51} \ L_{52} \ L_{53} \ L_{54} \ L_{55}] \rightarrow N'_y \end{aligned}$$

The transfer function from $[q]$ to $[q']$ ($G_{qq'}$) has to be evaluated with the $[N_z \ p \ r \ N_y]$ to $[N'_z \ p' \ r' \ N'_y]$ loop closed. The bound on $|G_{qq'}|$ can be obtained in two steps by closing two loops at a time, reducing it to two 3×3 cases.

The 3×3 transfer function G from $[q \ N_z \ p]$ to $[q' \ N'_z \ p']$ with the $[r \ N_y]$ to $[r' \ N'_y]$ loops closed is given by

$$G = G_{11} + G_{12}(I - G_{22})^{-1}G_{21}$$

where

$$\begin{aligned} G_{11} &= \begin{bmatrix} L_{11} & L_{12} & L_{13} \\ L_{21} & L_{22} & L_{23} \\ L_{31} & L_{32} & L_{33} \end{bmatrix}, \quad G_{12} = \begin{bmatrix} L_{14} & L_{15} \\ L_{24} & L_{25} \\ L_{34} & L_{35} \end{bmatrix} \\ G_{21} &= \begin{bmatrix} L_{41} & L_{42} & L_{43} \\ L_{51} & L_{52} & L_{53} \end{bmatrix}, \quad I - G_{22} = \begin{bmatrix} 1 - L_{44} & -L_{45} \\ -L_{54} & 1 - L_{55} \end{bmatrix} \\ (I - G_{22})^{-1} &= \begin{bmatrix} \frac{1}{(1-L_{44}) - \frac{L_{54}L_{45}}{1-L_{55}}} = F_{11}(L_{ij}) & \frac{L_{45}}{(1-L_{44})(1-L_{55}) - L_{54}L_{45}} = F_{12}(L_{ij}) \\ \frac{L_{54}}{(1-L_{44})(1-L_{55}) - L_{54}L_{45}} = F_{21}(L_{ij}) & \frac{1}{(1-L_{55}) - \frac{L_{54}L_{45}}{1-L_{44}}} = F_{22}(L_{ij}) \end{bmatrix} \\ G &= \begin{bmatrix} G_{11}(L_{ij}) & G_{12}(L_{ij}) & G_{13}(L_{ij}) \\ G_{21}(L_{ij}) & G_{22}(L_{ij}) & G_{23}(L_{ij}) \\ G_{31}(L_{ij}) & G_{32}(L_{ij}) & G_{33}(L_{ij}) \end{bmatrix} \\ &= \begin{bmatrix} L_{11} & L_{12} & L_{13} \\ L_{21} & L_{22} & L_{23} \\ L_{31} & L_{32} & L_{33} \end{bmatrix} + \begin{bmatrix} L_{14} & L_{15} \\ L_{24} & L_{25} \\ L_{34} & L_{35} \end{bmatrix} \begin{bmatrix} F_{11} & F_{12} \\ F_{21} & F_{22} \end{bmatrix} \begin{bmatrix} L_{41} & L_{42} & L_{43} \\ L_{51} & L_{52} & L_{53} \end{bmatrix} \end{aligned}$$

Using results from [7] for the 3×3 case, it follows that if the following conditions are satisfied

$$|L_{44}| + \frac{|L_{54}||L_{45}|}{1 - |L_{55}|} < 1 \quad (1a)$$

and

$$|L_{55}| < 1 \quad (1b)$$

then

$$|G_{kl}(L_{ij})| \leq G_{kl}(|L_{ij}|), \quad \text{for } k, l = 1, 2, 3$$

Because the magnitudes of L_{ij} 's for each frequency are known, one can easily calculate $G_{kl}(|L_{ij}|)$, and this will be a bound on $|G_{kl}(L_{ij})|$ if Eq. (1) is satisfied. Next, if

$$|G_{22}| + \frac{|G_{32}||G_{23}|}{1 - |G_{33}|} < 1 \quad (2a)$$

and

$$|G_{33}| < 1 \quad (2b)$$

one can compute a bound on the magnitude of the $G_{qq'}$ transfer function with the $[N_z \ p]$ to $[N'_z \ p']$ loop closed as well.

Note that the conditions (1) and (2) are not very restrictive and are satisfied in general for the problem of designing notch filters for gain stabilization. From a small gain theorem, the conditions (1b) and (2b) imply that the system is stable with only the third loop closed. This should normally be valid because only scalar sums are considered. Similarly, the conditions (1a) and (2a) imply that the system is stable with the second and third loops closed (in terms of scalar sums). This is also expected to be true in general.

Table 1 Weight selection and corresponding phase lags in each sensor path

Phase lag calculation at all sensor channels using Bode's integral						
Serial no	Cost function	q	Nz	P	R	Ny
A		Weighted attenuation				
1	[1 0 0 0 0]	10.34	67.12	69.99	57.72	66.55
2	[0 0 1 0 0]	66.83	60.62	8.766	62.62	49.955
3	[1 1 1 1 1]	14.67	1.27	11.49	4.22	2.12
\vdots	\vdots	\vdots	\vdots	\vdots	\vdots	\vdots
4	[1 0.065 0.45 0.08 0.008]	11.797	10.80	10.333	6.42	9.13
B		Variable weights				
1	[1 1 1 1 1]	11.99	8.78	10.70	8.79	6.74
2	[1.27 0.93 1.14 0.93 0.72]	11.64	11.728	11.14	11.35	10.77
3	[1.31 0.97 1.12 0.94 0.68]	11.60	11.735	11.38	11.53	11.28

III. Structural Filter Design Process

This section presents the two-step process for notch-filter design. The design proceeds by first finding out the optimal attenuation envelopes in each sensor path. In the second step, the individual notch-filter sections are designed for the optimal attenuation envelopes while minimizing the phase lag introduced by the notch filters at the rigid-body gain crossover frequency (~ 1 Hz).

A. Step 1: Design of Optimal Attenuation Envelopes

1. Weighted Attenuation

Let the attenuation required in each sensor path at a frequency (w_k) be denoted by

$$X_k = [m_q, m_{nz}, m_p, m_r, m_{ny}]$$

For a set of constant positive weighting parameters

$$W = [w_q, w_{nz}, w_p, w_r, w_{ny}]$$

the sum of the weighted attenuations is minimized at each discrete frequency point. The constrained optimization problem may be stated as follows: For each $w = w_k$, find an X_k that minimizes (W^*X_k), subject to all actuator and sensor margins ≥ 8 dB.

Optimal attenuation envelopes are obtained by collating the optimum attenuations at each frequency. Thus, for every set of weighting parameters, a set of optimum attenuation envelopes can be found out. The phase lag introduced by the notch filters in each of the sensor paths at 1 Hz can be readily found from the corresponding attenuation envelopes using Bode's gain-phase relationship [7]. The weights are adjusted in an iterative fashion to obtain acceptable phase lags in all the sensor paths. A few typical steps from the full design process are shown in item A in Table 1. The phase lag introduced by the notch filters in each of the sensor paths is also presented. The weights in items A.1 and A.2 in the table are selected as 1.0 for a specific channel and 0 for all the others. This gives the minimum phase lag attenuation required in the specific channel.

2. Variable Weights

The preceding method uses constant weights for obtaining the optimal attenuation envelopes. It is obviously possible to vary the weights in the cost function with frequency. At any discrete frequency point, "partial" phase lag contribution (at 1 Hz) can be computed from partial attenuation envelopes constructed using results available for all lower frequencies and assuming zero attenuation for all higher frequencies. The exponential of the weighted partial phase information can be used as weights for the current frequency point. If a particular sensor channel has a large partial phase lag as compared with the other channels, then the incremental phase increase in this channel should be minimized while letting the phase lag in the other sensor channels increase so long as it is possible to meet the design constraints. If the partial phase lag in all sensor channels till a frequency point w_k is represented as $\Phi_k = [\varphi_q \ \varphi_{nz} \ \varphi_p \ \varphi_r \ \varphi_{ny}]_k$, then the minimization problem is

restated: For each $w = w_k$, find an X_k that minimizes ($\exp(W^*\Phi_{k-1}) * [\Phi_k(X_k) - \Phi_{k-1}]$), subject to all actuator and sensor margins ≥ 8 dB.

The results are presented in item B of Table 1. The choice of the constant weight (W) is user selectable and may be varied to weigh specific sensor channels as deemed desirable for the problem at hand.

B. Step 2: Design of Individual Filter Sections

The values of the optimal attenuations over the entire frequency range generate five envelopes as Q_{env} , NZ_{env} , P_{env} , R_{env} , and NY_{env} , with an associated theoretical limit of the minimum phase lag achievable at 1 Hz, as discussed in the previous section. Figure 3 shows a plot of computed attenuation requirements of four digital notch filters in the inertial sensor paths. The dashed lines represent the optimal attenuation envelopes in the figure. Individual notch filters for each sensor path are designed with multiple filter sections to minimize the net phase lag at 1 Hz and simultaneously satisfy the optimal attenuation envelope constraint. Each filter section is represented as a second-order filter

$$TF = \frac{(1/\omega_n)^2 s^2 + 2(\zeta_n/\omega_n)s + 1}{(1/\omega_d)^2 s^2 + 2(\zeta_d/\omega_d)s + 1}$$

where ω_n and ω_d are the numerator and denominator frequencies, and ζ_n and ζ_d are the numerator and denominator damping coefficients. For example, the k th second-order filter section requires four parameters ($F_k = [\omega_n, \zeta_n, \omega_d, \text{ and } \zeta_d]_k$) to be tuned. Thus, the Q -structural filter design problem may be posed as follows: Find $F = [F_1, F_2 \dots F_N]$, corresponding to the Q filter [$Q_F = F_1, F_2 \dots F_N$], where N is the number of filter sections.

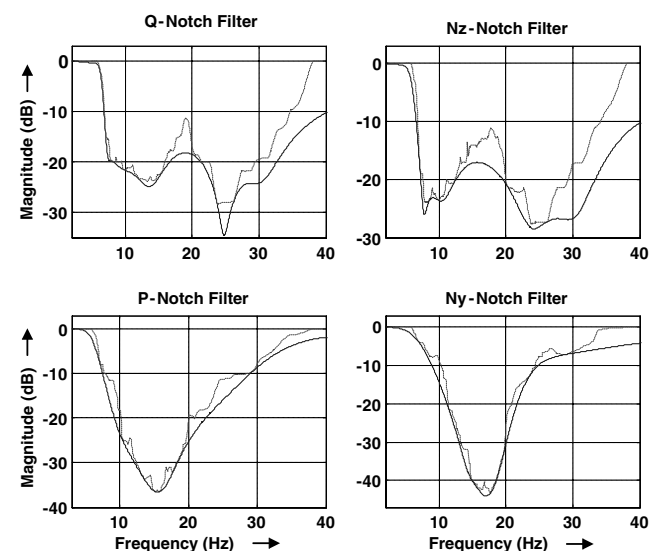


Fig. 3 Notch filters in sensor paths vis à vis required attenuation.

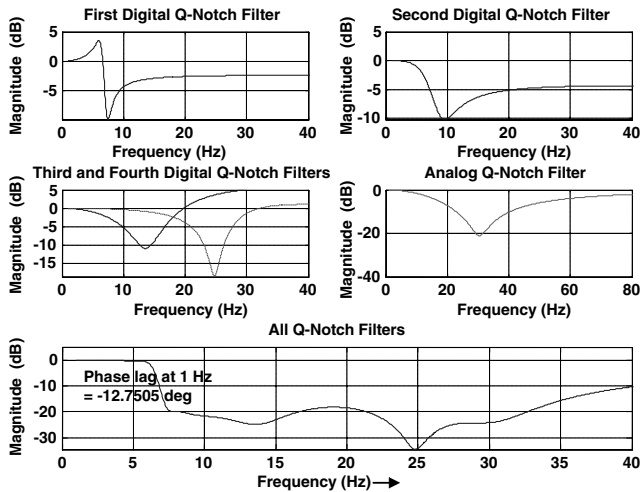


Fig. 4 Plots of individual filter sections for the Q -notch filters.

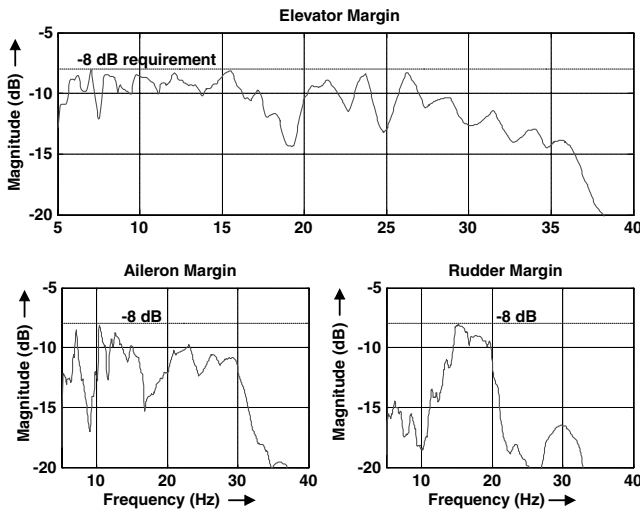


Fig. 5 Margin plots at the actuator consolidation points.

The minimum phase lag at 1 Hz (X) is subject to the following:

- 1) $Q_F < Q_{env}$: The attenuation of the designed filter is more than the optimal envelope.
- 2) $\zeta_n < \zeta_d$: Each filter section looks like a notch.
- 3) $|F_i| < 10$ dB, for $i = 1, 2, \dots, N$: The filter bounce back at high frequencies is limited.
- 4) $|Q_F| < 0.01$ dB: The overall signal amplification is limited.

This optimization problem is solved using standard MATLAB® routines. The results for some notch-filter designs (with combined digital and analog filter sections) are presented in Fig. 3. The solid lines are obtained from the filter design exercise. It can be seen that the filter frequency response grazes the attenuation envelope as closely as possible, especially at lower frequencies. The gain plots of the individual filter sections for the Q_F are shown in Fig. 4. From the plots it can be observed that the low frequency gain of each filter section is 0 dB. This ensures noninterference with the control law gains over the rigid-body bandwidth. The actuator margins are evaluated after designing all five structural filters, as presented in Fig. 5, and show that the military specification for the structural frequency range is satisfied.

C. Selection of the Number of Filter Sections

The individual notch-filter design was carried out with multiple filter sections in each of the five inertial feedback (q , N_z , p , r , and N_y) channels. The variation in the additional phase lag at 1 Hz introduced by the Q -structural filter with the number of filter sections is shown in Fig. 6. It is observed that as the number of filter sections is increased, the phase lag approaches the theoretical phase lag in the

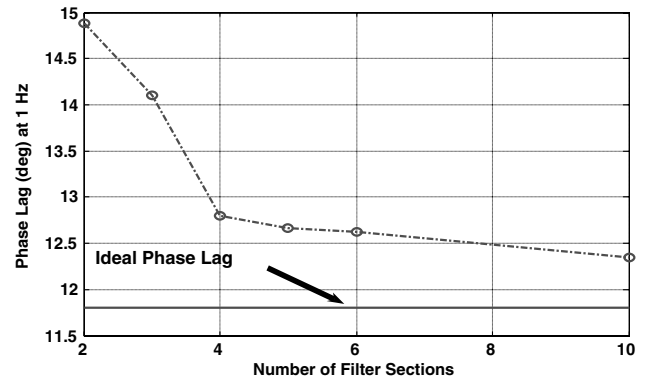


Fig. 6 Phase lag at 1 Hz vs number of filter sections for the Q -structural filter.

limit. This can be used as a guideline in selecting the number of filter sections. In practice, the number of filter sections required can be frozen when the addition of one more section does not improve the phase lag significantly.

IV. Conclusions

An elegant two-step process for the optimal design of notch filters for a multi-input, multi-output system with significant interaxis coupling to achieve gain stabilization is presented. The design emphasis is on minimizing phase lag at rigid-body gain crossover frequencies while meeting the structural stability margin requirement of 8 dB as required by MIL-F-9490D. In the first step, the optimal attenuation envelopes are obtained by trading off phase lags between the various sensor channels. The individual notch filters for each sensor path are designed in the second step. The use of Bode's integral to estimate the theoretical phase lag from the gain response of a filter significantly accelerates the first step and also helps in identifying the optimum number of filter sections required in each sensor path. A priori knowledge of the number of filter sections in a sensor path is not required; instead, it can be selected based on a tradeoff study between the computational load and an acceptable phase lag.

References

- [1] "Military Specification Flight Control Systems – Design, Installation and Test of Piloted Aircraft General Specification," U.S. Department of Defense, Rept. MIL-F-9490D, Washington, D.C., 5 Oct. 1992.
- [2] Chakravarthy, A., Deodhare, G., Patel, V. V., and Saraf, A., "Design of Notch Filters for Structural Responses with Multiaxis Coupling," *Journal of Guidance, Control, and Dynamics*, Vol. 22, No. 2, pp. 349–357, March–April 1999.
- [3] Mehra, R. K., Arambel, P. O., Sampath, A. M., Prasanth, R. K., and Parham, T. C., "On-Line Identification, Flutter Testing and Adaptive Notching of Structural Mode Parameters for V-22 Tilt Rotor Aircraft," *Sadhana*, Vol. 25, Pt. 2, April 2000, pp. 137–158. doi:10.1007/BF02703755
- [4] Le Garrec, C., and Kubica, F., "In-Flight Structural Modes Identification for Comfort Improvement by Flight Control Laws," *Journal of Aircraft*, Vol. 42, No. 1, 2005, pp. 90–92. doi:10.2514/1.3733
- [5] Halsey, S. A., and Goodall, R. M., "Kalman Filtering for Structural Coupling," Electronic Systems and Control Division Research, Department of Electronic and Electrical Engineering, Loughborough University (Great Britain), <http://www.lboro.ac.uk/departments/el/research/scg/pdfs/Halsey.pdf>, pp. 1–3 [retrieved 23 Jan. 2008].
- [6] Hoffmann, F., "FCS Notch-Filter Design Using Genetic/Evolutionary Algorithms," *AIAA Guidance, Navigation, and Control Conference*, AIAA, Reston, VA, Aug. 2004, pp. 16–19; also AIAA Paper 2004-4758.
- [7] Rajesh V., Singh, G. K., Deodhare, G., Patel, V. V., and Chetty, S., "Bode Integral Based Design of Notch Filters for Structural Coupling," *Proceedings of the International Conference on Advances in Control and Optimization of Dynamical Systems (ACODS-2007)*, Feb. 2007, pp. 323–331; also http://www.aero.iisc.ernet.in/acods2007/ppt/papers/323-R10_P215.pdf, pp. 323–331, [retrieved 9 June 2008].